Available online at www.sciencedirect.com

jmr&t Journal of Materials Research and Technology

www.jmrt.com.br

Original Article

Investigation of microstructural influence on entropy change in magnetocaloric polycrystalline samples of NiMnGaCu ferromagnetic shape memory alloy

E. Villa[a,*], C. Tomasi[b], A. Nespoli[a], F. Passaretti[a], G. Lamura[c], F. Canepa[d]

[a] Consiglio Nazionale delle Ricerche – Istituto della Materia Condensata e di Tecnologie per l'Energia (CNR-ICMATE Sede di Lecco) via G. Previati 1/e, 23900 Lecco, Italy

[b] Consiglio Nazionale delle Ricerche – Istituto della Materia Condensata e di Tecnologie per l'Energia (CNR-ICMATE Sede di Genova) Area della Ricerca di Genova, Via De Marini 6, 16149 Genova, Italy

[c] CNR-SPIN Corso Perrone 24, 16152 Genova, Italy

[d] Dipartimento di Chimica e Chimica Industriale, Università di Genova, via Dodecaneso 31, 16146 Genova, Italy

ARTICLE INFO

Article history:
Received 17 October 2019
Accepted 18 December 2019
Available online 30 December 2019

Keywords:
Magnetic Shape Memory Alloys
Calorimetric investigation
Thermoelastic martensitic transition
Magnetocaloric effect
Thermal treatment
NiMnGaCu

ABSTRACT

Among NiMnGa-based quaternary systems, NiMnGaCu exhibits an interesting giant magnetocaloric effect thanks to the temperature overlapping of magnetic transition and thermoelastic martensitic transformation (TMT), in particular for compositions with ≈6 at% Cu content. In the present work polycrystalline alloy samples with $Ni_{50}Mn_{18.5}Cu_{6.5}Ga_{25}$ chemical composition were prepared. We present an extensive calorimetric and structural characterization to explore the correlation between microstructural properties and magnetocaloric response induced by means of selected thermal treatments, likely driven by the contribution of TMT to the magnetocaloric effect. Our results give important hints on how the efficiency of the martensitic transition and its modulation in temperature has a final effect on the total ΔS change.

1. Introduction

During the last decades the research on magnetocaloric materials has attracted worldwide increasing attention thanks to their potential application in ecofriendly room-temperature refrigeration devices by replacing conventional gas compression/expansion technology [1]. Consequently, a large number of studies on magnetic materials showing large Magneto Caloric Effect (MCE) near room temperature have been published [2].

The magnetocaloric effect is usually expressed in terms of adiabatic temperature change (ΔT_M) and isothermal entropy change (ΔS_M) to quantify the caloric effect. The so called Giant Magnetocaloric Effect (GMCE), i.e., the high latent heat output of magnetic field driven phase transformation was first observed in $Gd_5(Si_{1-x}Ge_x)_4$ [3] and then in $La(Fe_xSi_{1-x})_{13}$ [4], $MnFeP_{1-x}As_x$ [5], $MnAs_{1-x}Sb_x$ [6] alloys.

* Corresponding author.
E-mail: elena.villa@cnr.it (E. Villa).

https://doi.org/10.1016/j.jmrt.2019.12.057

Among the classes of materials showing MCE, ferromagnetic shape memory alloys (FSMAs) are of great interest. In particular, NiMn-based metamagnetic shape memory alloys are known as an important class of magnetostructural multiferroics that exhibit large caloric effects. By heating (cooling), these alloys experience a structural transformation from (to) low temperature in low simmetry martensite phase (as tetragonal for example for NiMnGaCu) to (from) high temperature cubic austenite phase accompanied by a MCE and other functional properties such as shape memory effect. A large and sharp change in magnetization can be associated to the structural transformation and, thanks to possible coupling effects, giant effects can be attained.

When a third element is added to the metamagnetic NiMn-based alloys different magnetic behaviour can be obtained. In case of NiMnX (X = In, Sn, Sb), the Heusler structured austenite phase is ferromagnetic whereas the tetragonal martensite is paramagnetic or antiferromagnetic. Since the vibrational entropy in the austenite phase is higher than that in the martensite phase, the two entropic contribution, i.e. magnetic and vibrational, play a conflictual role during the phase transformation, leading in some case to lower total ΔS [7] ranging also to so-called Inverse MagnetoCaloric Effect (IMCE). However for NiMnX (X = In, Sn, Sb) also in condition for developing Inverse MagnetoCaloric effect we can obtain important value for ΔS [7].

Conversely, in some other NiMn-based alloys, e.g. the full Heusler Ni_2MnGa alloy, the austenite phase is low-magnetic while the martensite is high-magnetic. In such a case both ferroelastic and ferromagnetic effects give a positive coupling leading to a higher total ΔS [8] and to MCE. In this alloy the martensitic transformation takes place at $T_M = 188\,K$ and the Curie temperature, T_C, falls at 364 K. Some recent studies focused on the partial replacement of Mn by means of non-magnetic Cu with the purpose of tuning the transition temperatures and possibly overlapping T_M and T_C.

For instance, Mahmud Khan et al. [9] reported that the ferromagnetic ordering temperature rapidly decreases and the martensitic transition temperature rises by increasing Cu content. A systematic study on the composition dependence of the martensitic transformation and the magnetic transition temperatures of the martensite and the austenite phases in the system $Ni_{46}Mn_{25+x}Ga_{25-x}Cu_4$ alloys was carried out by Jiang et al. [10]. Further, the martensitic transition and its correlations with both microstructure and composition in $Ni_{56}Mn_{25+x}Cu_xGa_{19}$ ($x = 0, 1, 2, 4, 8$) high temperature FSMA (Ferromagnetic Shape Memory Alloys) was investigated by Ma et al. [11]. These authors found that the peak temperature of the martensitic transformation increases monotonically with x. Besides, for $x < 2$ a single tetragonal martensitic phase is observed whereas for $x \geq 2$ dual phase (martensite + fcc γ phase) compositions were found. Wang et al. [12] addressed their study on the martensitic transformation and mechanical properties of the single phase wide-hysteresis $Ni_{50}Mn_{25}Cu_{17}Ga_8$ shape memory alloy. Similarly, Li et al. [13] focused their attention on the single phase wide-hysteresis $Ni_{50}Mn_{25}Cu_{25-x}Ga_x$ ($x = 3$–10) FSMA where a survey on the martensitic transformation, the mechanical properties, the shape memory behaviour as well as a microstructure study was presented. Investigations about magnetocaloric aspects on NiMnCuGa alloys were considered by various research groups [14,15]. Stadler et al. [14] reported the magnetocaloric properties of $Ni_2Mn_{1-x}Cu_xGa$ substituted Heusler alloy on the basis of magnetization measurements. A maximum entropy change, ΔS_M, of $-64\,J/kg\,K$ was found at $T = 308\,K$ for a field change, $\mu_0\Delta H$, of 5 T. It was also demonstrated that ΔS_M changes pretty linearly with ΔH and that subtle variations of composition reflect onto the temperature at which ΔS_M occurs. Later, Sarkar et al. [15] obtained a ΔS_M, of $-81.8\,J/kg\,K$ at $T = 303\,K$ for a $\mu_0\Delta H$ of 9 T on the $Ni_{50}Mn_{18.5}Cu_{6.5}Ga_{25}$ FSMA by finely tuning the austenite transformation temperature to the ferromagnetic Curie temperature, T_C, during reverse martensitic transformation (heating cycle). Such a fine tuning was achieved by varying the amount of Cu since rising copper content resulted in an increase of the martensitic transformation temperature and a decrease of T_C. Zhan et al. [16] carried out a study on $Ni_{49.4}Mn_{26.1}Ga_{20.8}Cu_{3.7}$ microwires produced by melt-extraction for magnetocaloric applications. An excellent MCE was achieved by chemical ordering annealing that allowed to reach the magnetostructural coupling. In such a way, both internal stress and defects density due to the preparation process, which in turn lowered the saturation magnetization, were reduced. Recently, Zhao et al. [17] presented an investigation on $Ni_{50}Mn_{25-x}Cu_xGa_{25}$ ($x = 5.5$, 6, 6.5) where experimental results were analysed in the framework of the Landau model. They found that both magnetocaloric entropy change (ΔS_M) and elastocaloric temperature change (ΔT) increase with the Cu content, and maximum values of $\Delta S_M = 1.01\,J/mol\,K$ and $\Delta T = 8.1\,K$ are attained with $x = 6.5$ at $T \approx 305\,K$ for a $\mu_0\Delta H = 5.0\,T$. The authors stated that the physical origin behind the large MCE stems in the magnetoelastic coupling, i.e. the total caloric response in the NiMnGaCu SMAs depends on the strength of magnetoelastic coupling between lattice and magnetic freedoms.

The aim of the present work is to investigate how the TMT contribution affects the total MCE, and therefore how the magnitude of this effect is related to the modulation of the microstructure [16].

2. Experimental

Starting from pure (>99%) metallic elements, small ingot buttons of $Ni_{50}Mn_{18.5}Cu_{6.5}Ga_{25}$ (in at. %) were prepared in a non-consumable electrode vacuum arc furnace (Leybold LK6/45). The ingots were melted into a water-cooled copper crucible, under protective atmosphere (pure 99,999 Ar). The melting procedure was repeated six times to improve chemical homogeneity. In the first thermal treatment (TT) the as grown samples were annealed at 1123 K for 6 h under vacuum conditions, followed by slow cooling (≈1 K/min) to room temperature. In order to modulate the microstructure, further different TT at 1123 K were applied to distinct aliquots: i) 6 and 18 h in inert atmosphere followed by water quenching (WQ samples), ii) 6 and 18 h under vacuum followed by slow quenching (SC samples). Therefore, each sample under investigation has been named with a string that joints the time duration of the second TT (6 h, 12 h, 24 h) and how the temperature was reduced (SC or WQ). A brief description of the sample investigated in the present work with the corre-

Table 1 – Summary of the second thermal treatment (TT) on the investigated samples.

Sample	Thermal treatment
6 hSC	Homogenization for 6 h in vacuum followed by slow cooling
12 hWQ	Homogenization + TT for 6 h in Ar followed by water quench
24 hWQ	Homogenization + TT for 18 h in Ar followed by water quench
12 hSC	Homogenization + TT for 6 h in vacuum followed by slow cooling
24 hSC	Homogenization + TT for 18 h in vacuum followed by slow cooling

sponding second thermal treatment at 1123 K is summarized in Table 1.

The calorimetric analysis was performed by a differential scanning calorimeter (DSC) Q100 TA Instruments, fitted with a liquid nitrogen cooling system from [223 K; 370 K] temperature range at a rate of 10 K/min. The characteristic temperatures measurements for martensitic and reverse transitions were obtained using the tangent method intersection between the tangent of the base line and the tangent at the peak inflection point. The enthalpies values were obtained by integration of the complete peak transition. Specific heat capacity (Cp) measurements were collected by means of Modulated DSC (MDSC) using the same equipment under quasi-isothermal conditions. Microscopic analysis (OM) on polished samples was obtained using a Leitz-ARISTOMET light microscope. The compositional analysis of each sample was assessed by Energy Dispersive X-ray Spectrometer (EDS, INCA ENERGY 200 Oxford Instr.) connected to a Scanning Electron Microscope (SEM LEO 1430). Besides, optical microscopy (OM) images of mechanically polished samples were obtained using a Leitz-ARISTOMET light. Before OM observations, samples were chemically etched with Marble's reagent for 30 s. X-ray diffraction (XRD) patterns were recorded on bulky polycrystalline samples at different temperature in the [273 K; 373 K] temperature range, by the X-ray diffractometer Panalytical XPert PRO with theta-2theta alignment. Magnetization measurements were performed by a commercial DC-SQUID magnetometer MPMS2 by Quantum Design in the temperature range 300 K < T < 360 K and applied magnetic fields up to 5.5 T.

3. Results

The sample stoichiometry formula was successfully determined by EDS to be $Ni_{50.3}Mn_{18,2}Cu_{6.6}Ga_{24.9}$ at%, and in good agreement with the nominal composition considering the accuracy of the EDS technique. Fig. 1 shows the images recorded by optical microscopy on all investigated samples. Unfortunately, the intrinsic high brittleness of the material does not allow to completely remove sample scratches and, hence, to obtain better quality pictures. In any case, the images reported in Fig. 1 can give a first clue about the grain structure. For the "slow cooling" samples at room temperature, the presence of large and anisotropic grains with visible martensitic lamellae structure can be easily observed. Such an anisotropic grain growth could be likely ascribed to a preferential growing along the cooling direction during the sample preparation. Conversely, the grain structure obtained in "water quenched" samples looks more isotropic although inter-granular separations and cracking effects are more evident.

The DSC analysis was performed in three consecutive thermal cycles to have a first control of thermal stability TMT. The modulation of the microstructure plays two main effects on TMT: i) it modifies the TMT and Tc transition temperatures and ii) it changes the shape and area of transformation peaks which, in turn, are directly related to the enthalpies involved in the process. The enthalpic effects involved in the martensitic transformation contribute to the total entropy change which is the main parameter indicating the caloric performance. It is not wrong to observe that the evaluation of the correlated enthalpies is not adequate to exhaustively describe the effect of the contribution of TMT to a total change in entropy. Hence, a new parameter strictly related to the *calorimetric efficiency* (CE_f (J/K) in the following) of the TMT should be considered. It can be expressed as the ratio between the enthalpy change, ΔH, and the half width at the full maximum (HWFM) of the transition peak ΔT: $CE_f = \Delta H/\Delta T$. Further, the entropy change during TMT, ΔS_{TMT}, is calculated as the ΔH to T_0 ratio, where Af is the Austenite phase finish temperature and Ms is the Martensitic phase start temperature [18]:

$$T_0 = \frac{Af + Ms}{2}$$

In the following Figures, the average values for transformation temperatures, the enthalpy ΔH, and entropy change, ΔS_{TMT}, are shown. In the inset of Fig. 3 the elaborated efficiency coefficients CE_f are also reported.

All the examined samples exhibit good thermal stability and both transition temperatures and registered peaks are stable for three consecutive cycles, with discrepancies less than 1 K. In Fig. 2 the first cycle DSC traces of the investigated samples along with the average transformation temperatures for three consecutive thermal cycles are shown.

The examined samples generally exhibit transition temperatures a little higher than those published by Sarkar et al. [15], although the chemical composition checked by EDS is fairly close to what reported by these authors. Moreover, samples having the same chemical composition but different thermal treatment show a noticeable shift in transition temperatures. For instance, the sample 24 h WQ exhibits the lowest transformation temperatures and a highly structured peak shape appearance, a general feature of samples obtained by slow cooling and/or with thermal treatment time of 24 h. This broad transition smeared over a wide temperature range is probably due to the presence of distinct regions inside the material requiring different thermal energy extents to transform. Such an aspect is quite usual in Fe SMA's, named Jerkey structure of DSC [19] but in the present case the "distribution of the transition" is very emphasized and spreads over a large temperature interval (higher than 30 K). It can be observed by optical or SEM microscopy that both slow cooling and prolonged thermal treatments induce a separation into multiple martensitic domains inside the material, in some cases related also to intergranular unsticking by cracks or separations.

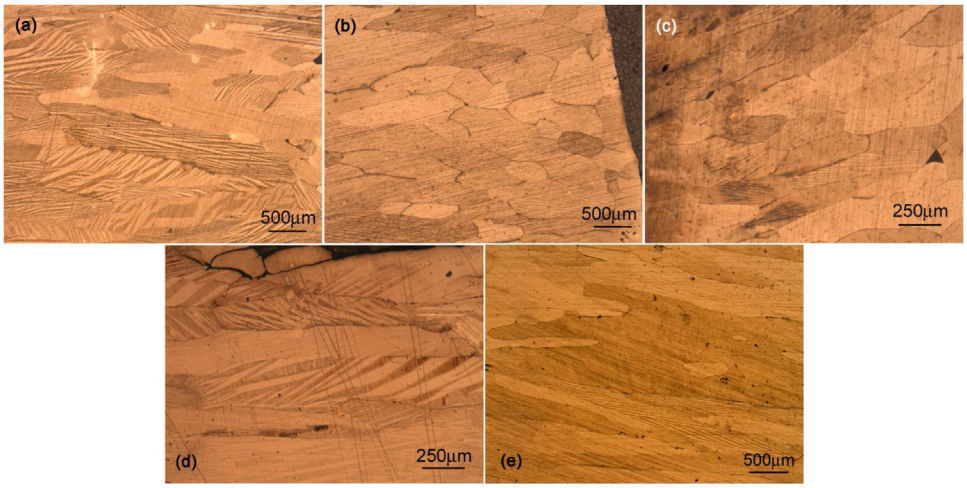

Fig. 1 – Optical microscopy images registered for all the samples: (a) 6 hSC; (b) 12 hWQ, (c) 24 hWQ; (d) 12 h SC; (e) 24 hSC.

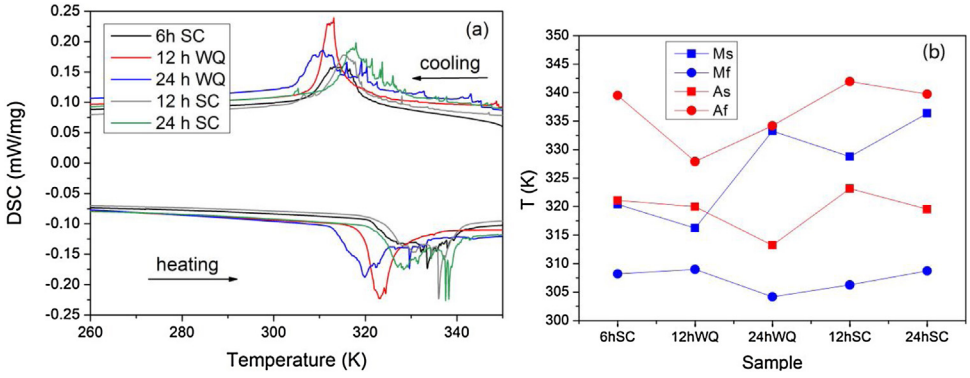

Fig. 2 – a) DSC analysis for the first cycle of all the studied samples and b) average registered transition temperatures: Ms = Martensite start temperature, Mf = Martensite finish temperature, As = Austenite start temperature, Af = Austenite finish temperature.

Among the investigated samples, the specimen 12 h WQ exhibits the narrowest transition and the sharpest calorimetric peak although the corresponding enthalpy of transformation is not the highest. In fact, in this sample the transition looks more homogeneous and takes place in a shorter temperature range as confirmed by the elaborated efficiency coefficient depicted in Fig. 3, where sample 12 h WQ presents the highest value.

On the basis of calorimetric analysis, the sample 12 h WQ has been considered for a deeper calorimetric characterization. Fig. 4 depicts the behavior of the Specific Heat Capacity obtained by MDSC. The dots (on cooling) and the squares (on heating) represent the average values between two measurements recorded by applying temperature sinusoidal waves with two different periods (100 s and 120 s) and an amplitude of ±0.5 K.

The results obtained by quasi-isothermal Cp measurements are in good agreement with the DSC analysis of Fig. 3. By considering a reasonable experimental error of ±5%, taking into account both the sample shape and the different paths in experimental heat transmission, a good correspondence between the values obtained in heating and cooling part of the measurements is found over Af temperature. Conversely, in the martensitic phase the effect of the thermal cycling gives rise to a remarkable difference in the Cp measured values, maybe due to dislocation defects introduced by the thermal treatment during the nucleation and growth of martensitic twins domains.

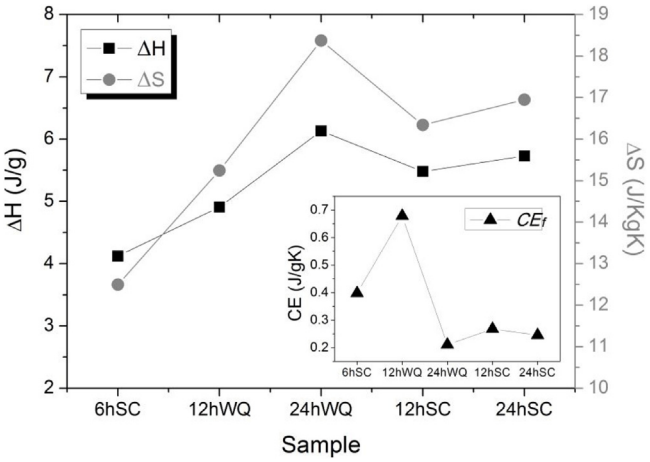

Fig. 3 – Enthalpies and entropies changes during TMT registered by DSC. In the inset the CE_f parameter for the samples investigated is shown.

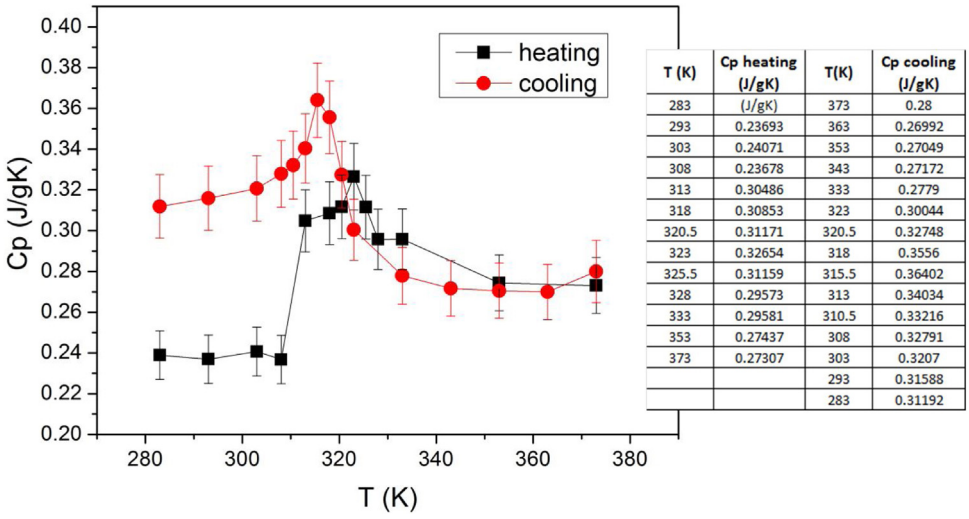

T (K)	Cp heating (J/gK)	T(K)	Cp cooling (J/gK)
283	(J/gK)	373	0.28
293	0.23693	363	0.26992
303	0.24071	353	0.27049
308	0.23678	343	0.27172
313	0.30486	333	0.2779
318	0.30853	323	0.30044
320.5	0.31171	320.5	0.32748
323	0.32654	318	0.3556
325.5	0.31159	315.5	0.36402
328	0.29573	313	0.34034
333	0.29581	310.5	0.33216
353	0.27437	308	0.32791
373	0.27307	303	0.3207
		293	0.31588
		283	0.31192

Fig. 4 – Heat Capacity vs temperature of sample 12 hWQ measured by MDSC in quasi isothermal conditions on heating and cooling sequences. The error bars reported correspond to an error of 10%.

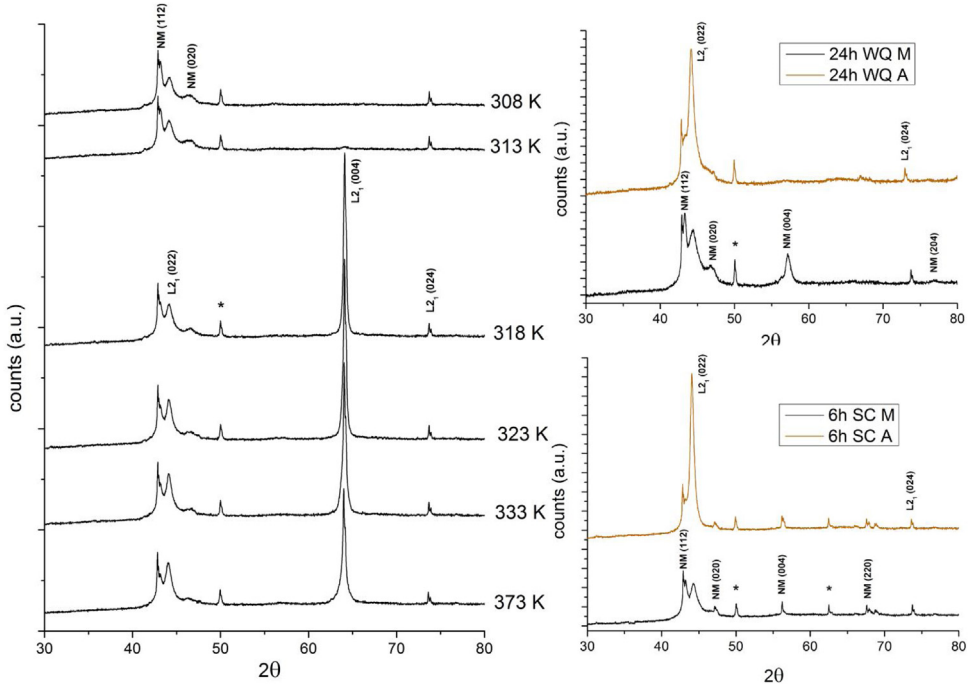

Fig. 5 – a) XRD pattern recorded on sample 12 hWQ at different temperatures. (b) and c) XRD patterns recorded on sample 24 hWQ and 6 hSC, respectively at temperatures: Mf −10 K and Af+10 K. The reflections marked by * belong to sample holder.

In order to check the crystalline phases in the sample 12 h WQ as well as the phase ratio at different temperatures, isothermal XRD scans on austenite and martensite at temperature steps of 5 K (on cooling) were performed. The samples investigated were in the bulk form to avoid changes in their original grain structure. Therefore, the recorded patterns exhibit different intensity ratios among their peaks according to different texture and preferential grain orientation. From a first glance, in Fig. 5 one can easily observe the presence of $L2_1$ structure peaks ascribed to austenite and modulated peaks of martensite. For the sake of clarity, we consider only the diffraction patterns recorded on 6 hSC, 24 hWQ and 12 hWQ. In all the registered patterns the co-existence of two crystallographic phases is found. Besides, in samples obtained by slow cooling, there is no evidence of the γ phase [20,21], in particular for sample 12 hWQ the XRD pattern evolution confirms a rapid structural change with the complete disappearance of the $L2_1$ (004) austenitic peak within the chosen minimum T-step width.

We used magnetization measurement at different temperature and magnetic fields to obtain an evaluation of change in Entropy ΔS vs Temperature [22]. In the following Fig. 6 we report the results, the measurements have been carried out in heating therefore the change in entropy measured is negative. The magnetization curves have been registered with a temperature step of 2 K in the transformation range and the

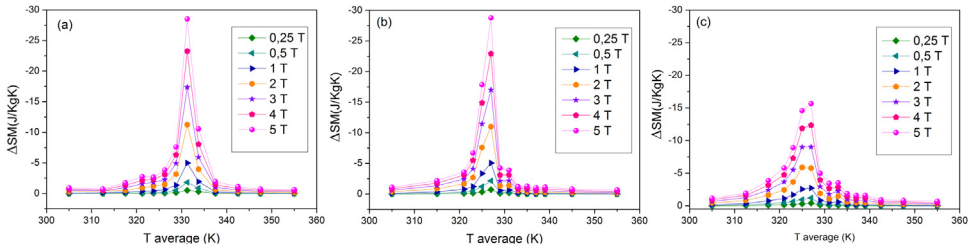

Fig. 6 – ΔS measured for (a) 6 hSC; (b) 12 hWQ and (c) 24 hWQ.

values of ΔS have been obtained by integration of these curves at fixed temperature. The evolution of ΔS is reported for the samples 6 hSC, 24 hWQ and 12 hWQ in Fig. 6.

4. Discussion

The high brittleness of FSMA encumbers the manufacturing of different microstructured materials by mean of canonical hot and cold deformation processes. Therefore, in the present work, the microstructure modulation in the NiMnGaCu alloy was accomplished by applying suitable thermal treatments at 1173 K for different amounts of time and well defined cooling procedures. When the microstructure is described and investigated, it is important to stress that attention is mainly focused on grain structure, grain boundaries as well as on the presence and distribution of defects. All the above mentioned features are modulated by thermal treatment and strongly affect the TMT. The effect of these treatments on the sample microstructure were observed by optical microscopy (OM). In Fig. 1 we show that the main effect of slow cooling is the creation of an anisotropic grain structure with long grains where the martensitic twins form in large domain and are well visible. In the water-quenched samples the grain structure looks more isotropic with smaller grains where the martensitic phase appears as thin martensitic lamellae.

For all the examined samples, in particular for the water-quenched ones, the effect of the above mentioned brittleness displays in form of grains separation and presence of frequent cracks. The direct outcome of these different grain structures can be estimated by calorimetric analysis. In fact, the thermoelastic martensitic transformation directly is influenced by the presence of energy barriers, by the structural homogeneity of the alloys during the formation and shrinking of the martensitic domains vs temperature. This aspect is directly reflected in the DSC thermograms, in the shape and width of the peak transition, in their temperature position and in the measured enthalpies [19,23,24].

As reported in Figs. 2 and 3, the TMT measured by DSC can be considered from different points of view. The TMT position, the overlapping with Tc and the transformation efficiency influenced the related entropy contribution to a total entropy change during the magnetocaloric effect. In other words, the modulation of microstructure improves the capability of the material to give a quick energy contribution in the entropy change to obtain a final improved change ΔT in the magnetocaloric application devices. According to Figs. 2 and 3, the samples 24 h WQ, 12 h SC, and 24 h SC exhibit the highest values both in ΔS and ΔH of transition but the transformation efficiency, calculated on the basis of the individuated parameters, is the lowest. The previous calorimetric investigation of the thermal properties on the more promising sample 12 hWQ indicates a behavior of Cp value with very narrow hysteresis and this set of values is reported in Fig. 4.

The XRD analysis is in good agreement with the results reported in literature, although in the present work the diffraction patterns show a noticeable existence of residual martensite in parent phase. This suggest that it is possible to tailor specific thermal treatment to avoid this blocked martensitic zone in austenite and it possible to further improve this work of optimization of microstructure, increasing in this way the material involved in the transformations and therefore the contribution of TMT in the total change in ΔS_{TOT}.

In Fig. 6 the results of magnetic entropy change vs temperature obtained by magnetization measurements at different applied magnetic fields are reported.

The selected samples are the most significant ones to make an interesting comparison on the basis of considerations about the efficiency of the martensitic transition: the sample 24 hWQ has the highest ΔS_{TMT} but the lowest CE_f, contrarily the samples 12 hWQ has the highest CE_f and lowest ΔS_{TMT}. The sample 6 hSC has the lowest ΔS in TMT and an intermediate value in CE. Therefore, the CE_f coefficient gives a better description of how the contribution of the entropy change due to TMT (ΔS_{TMT}) affects the total ΔS involved in the magnetocaloric effect. In fact, ΔS_{TMT} itself is not a suitable parameter to express the efficiency of the TMT contribution, in particular when a transition is not sharp but smeared over a wide range of temperature. The quick contribution in a small range in temperature seems to have better effect, therefore the CE_f coefficient can be useful to foresee the best performance in magnetocaloric response. As can be seen, the ΔS obtained by the magnetization curves vs T at different Magnetic Fields denotes that the CE is the main parameter affecting the total entropy change. In fact, the sample 6 hSC and chiefly the sample 12 hWQ exhibit the highest magnetic ΔS values, around −30 J/KgK at a magnetic field of 5 T. It is worth noting that for the sample 6 hSC there is also a shift of the ΔS peak to higher temperatures which may be associated to a better overlapping between Tc and the transition temperature TMT. For the sample 24 hSC the magnetic ΔS value reduces considerably to about −15 J/KgK at a magnetic field of 5 T. Hence, albeit this latter sample has the highest ΔS value in TMT, the total entropy change does not result the highest. Conversely, the CE_f plays

a more important role and the efficiency of the TMT has a big influence on the total entropy change. A more efficient TMT is related to an improvement of microstructure which might give a better magnetoelastic coupling between lattice and magnetic freedoms. Therefore, a deeper investigation on the microstructure and the exploration of possible thermo-mechanical processes to improve the homogeneity and the quality of martensitic transition is an interesting way to be considered to improve the final magnetocaloric performance in FSMA.

A future completion of this first indication, with measurements of heat capacity under magnetic field and finally of Maximum Refrigerant capacity (RCP) will give an exhaustive demonstration of this first step.

5. Conclusions

In this work the modulation of microstructure of the $Ni_{50}Mn_{18,5}Cu_{6.5}Ga_{25}$ alloy was investigated before and after different TT. The effect of TMT on the total entropy change, which is the base of the magnetocaloric effect, was studied and correlated to the CE_f parameter, which represents the efficiency of TMT. The indirect evaluation of magnetocaloric properties by magnetization measurements vs. temperature and magnetic field gives a clear indication that the modulation of microstructure can affect the magnetocaloric response by leading to possible overlapping of Tc and transition temperatures. In particular, the modulation of the structure acts on the efficiency of TMT which corresponds to a quick and effective contribution to the total ΔS and therefore to the overall caloric performance.

Conflicts of interest

The authors declare no conflicts of interest.

Appendix A. Supplementary data

Supplementary material related to this article can be found, in the online version, at doi:https://doi.org/10.1016/j.jmrt.2019.12.057.

REFERENCES

[1] Glanz J. Materials science - Making a bigger chill with magnets. Science 1998;279:2045.

[2] Balli M, Jandl S, Fournier P, Kedous-Lebouc A. Advanced materials for magnetic cooling: Fundamentals and practical aspects. Appl Phys Rev 2017;4:021305, http://dx.doi.org/10.1063/1.4983612.

[3] Pecharsky VK, Gschneidner KA Jr. Giant magnetocaloric effect in Gd-5(Si2Ge2). Phys Rev Lett 1997;78:4494.

[4] Wen GH, Zheng RK, Zhang XX, Wang WH, Chen JL, Wu GH. Magnetic entropy change in LaFe13-xSix intermetallic compounds. J Appl Phys 2002;91:8537.

[5] Brück E, Ilyn M, Tishin AM, Tegus O. Magnetocaloric effects in MnFeP1-xAsx-based compounds. J Magn Magn Mater 2005;290:8.

[6] Wada H, Morikawa T, Taniguchi T, Shibata T, Yamada Y, Akishige Y. Giant magnetocaloric effect of MnAs1-xSbx in the vicinity of first-order magnetic transition. Phys B 2003;328:114.

[7] Biswas A, Chandra S, Samanta T, Phan MH, Das I, et al. he universal behavior of inverse magnetocaloric effect in antiferromagnetic materials. J Appl Phys 2013;113:17A902, http://dx.doi.org/10.1063/1.4793768.

[8] Gomes AM, Khan M, Stadler S, Ali N, Dubenko I, Takeuchi AY, Guimarães AP. Magnetocaloric properties of the Ni2Mn1-x(Cu,Co)(x)Ga heusler alloys. J Appl Phys 2006;99:08Q106, http://dx.doi.org/10.1063/1.2164415.

[9] Khan M, Dubenko I, Stadler S, Ali N. The structural and magnetic properties of Ni2Mn1-x M x Ga (M=Co, Cu). J Appl Phys 2005;97:10M304, http://dx.doi.org/10.1063/1.1847131.

[10] Jiang C, Wang J, Li P, Jia A, Xu H. Search for transformation from paramagnetic martensite to ferromagnetic austenite: NiMnGaCu alloys. Appl Phys Lett 2009;95:012501, http://dx.doi.org/10.1063/1.3155199.

[11] Ma Y, Yang S, Jin W, Liu X. Ni56Mn25-xCuxGa19 (x=0, 1, 2, 4, 8) high-temperature shape-memory alloys. J Alloys Compd 2009;471:570–4, http://dx.doi.org/10.1016/j.jallcom.2008.07.016.

[12] Ma Y, Yang S, Jin W, n Liu X. Ni56Mn25-xCuxGa19 (x=0, 1, 2, 4, 8) high-temperature shape-memory alloys. J Alloys Compd 2009;471:570–4, http://dx.doi.org/10.1016/j.jallcom.2008.07.016.

[13] Li Y, Wang J, Jiang C. Study of Ni-Mn-Ga-Cu as single-phase wide-hysteresis shape memory alloys. Mater Sci Eng A 2011;528:6907–11, http://dx.doi.org/10.1016/j.msea.2011.05.060.

[14] Stadler S, Khan M, Mitchell J, Ali N, Gomes AM, Dubenko AY, Guimarães AP. Magnetocaloric properties of NMn1-xCuxGa. Appl Phys Lett 2006;88:192511, http://dx.doi.org/10.1063/1.2202751.

[15] Sarkar SK, Sarita, Babu PD, Biswas A, Siruguri V, Krishnan M. Giant magnetocaloric effect from reverse martensitic transformation in Ni-Mn-Ga-Cu ferromagnetic shape memory alloys. J Alloys Compd 2016;670:281–8, http://dx.doi.org/10.1016/j.jallcom.2016.02.039.

[16] Zhang X, Qian M, Zhang Z, Wei L, Geng L, Sun J. Magnetostructural coupling and magnetocaloric effect in Ni-Mn-Ga-Cu Microwires. Appl Phys Lett 2016;108:052401, http://dx.doi.org/10.1063/1.4941232.

[17] Zhao D, Castán T, Planes A, Li Z, Sun W, Liu J. nhanced caloric effect induced by magnetoelastic coupling in NiMnGaCu Heusler alloys: Experimental study and theoretical analysis. Phys Rev B 2017;96:224105, http://dx.doi.org/10.1103/PhysRevB.96.224105.

[18] Khovailo VV, Oikawa K, Abe T, Takagi T. Entropy change at the martensitic transformation in ferromagnetic shape memory alloys Ni2+xMn1-xGa. J Appl Phys 2003;93:8483, http://dx.doi.org/10.1063/1.1556218.

[19] Nespoli A, Biffi CA, Villa E, Tuissi A. Effect of heating/cooling rate on martensitic transformation of NiMnGa-Co high temperature ferromagnetic shape memory alloys. J Alloys Compd 2017;690:478–84, http://dx.doi.org/10.1016/j.jallcom.2016.08.143.

[20] Yang S, Liu Y, Wang C, Liu X. Martensite stabilization and thermal cycling stability of two-phase NiMnGa-based high-temperature shape memory alloys. Acta Mater 2012;60:4255–67, http://dx.doi.org/10.1016/j.actamat.2012.04.029.

[21] Santamarta R, Muntasell J, Font J, Cesari E. Thermal stability and microstructure of NieMneGaeCu high temperature shape memory alloys. J Alloys and Compd 2015;648:903–11, http://dx.doi.org/10.1016/j.jallcom.2015.07.054.

[22] Pecharsky VK, Gschneidner KA. Magnetocaloric effect from indirect measurements: Magnetization and heat capacity. J of Appl Phys 1999;86:565, http://dx.doi.org/10.1063/1.370767.
[23] Besseghini S, Pasquale M, Passaretti F, Sciacca A, Villa E. NiMnGa polycrystalline magnetically activated shape memory alloy: a calorimetric investigation. Scripta Mater 2001;44:2681–7.
[24] Albertini F, Besseghini S, Paoluzi A, Pareti L, Pasquale M, Passaretti F, Sasso CP, Stantero A, Villa E. Structural, magnetic and anisotropic properties of Ni2MnGa melt-spun ribbons. J Magn Magn Mat 2002;242-245:1421–4.